Opportunistic Energy Sharing Between Power Grid and Electric Vehicles: A Game Theory-Based Pricing Policy

Ankur Sarker[†], Zhuozhao Li[†], William Kolodzey[*], and Haiying Shen[†]
[†]University of Virginia, Charlottesville, VA 22904, USA
[*]Clemson University, Clemson, SC 29634, USA
[†]{as4mz,zl5uq,hs6ms}@virginia.edu, [*]wkolodz@clemson.edu

Abstract—Electric vehicles (EVs) have great potential to reduce dependency on fossil fuels. The recent surge in the development of online EV (OLEV) will help to address the drawbacks associated with current generation EVs, such as the heavy and expensive batteries. OLEVs are integrated with the smart grid of power infrastructure through a wireless power transfer system (WPT) to increase the driving range of the OLEV. However, the integration of OLEVs with the grid creates a tremendous load for the smart grid. The demand of a power grid changes over time and the price of power is not fixed throughout the day. There should be some congestion avoidance and load balancing policy implications to ensure quality of services for OLEVs. In this paper, first, we conduct an analysis to show the existence of unpredictable power load and congestion because of OLEVs. We use the *Simulation for Urban MObility* tool and hourly traffic counts of a road section of the *New York City* to analyze the amount of energy OLEVs can receive at different times of the day. Then, we present a game theory based on a distributed power schedule framework to find the optimal schedule between OLEVs and smart grid. In the proposed framework, OLEVs receive the amount of power charging from the smart grid based on a power payment function which is updated using best response strategy. We prove that the updated power requests converge to the optimal power schedule. In this way, the smart grid maximizes the social welfare of OLEVs, which is defined as mixed consideration of total satisfaction and its power charging cost. Finally, we verify the performance of our proposed pricing policy under different scenarios in a simulation study.

Index Terms—Electric vehicles; Online electric vehicles; Wireless power transfer; Smart grid; Power schedule; Game theoretic pricing policy;

I. INTRODUCTION

According to a recent study [1], todays transportation system mostly depends on petroleum-based energy consumption where automobiles and other highway vehicles contribute to high CO_2 emissions. In 2014, overall emissions from transportation activities increased by 17 percent. Electric vehicles (EVs) have great potential to reduce fossil fuel consumption. Several works already demonstrate the possible impact of EVs on the road transportation system [2–5] such as petroleum consumption reduction and environmental pollution reduction. As the total number of vehicles keeps rising, countries are urged to switch from gas-driven vehicles to EVs in order to decrease the consumption of fossil fuels. For example, Tesla Motors has launched the affordable "Model 3" EV on March 31, 2016 for mass production [6].

Since the onboard battery of an EV needs to meet the energy demands of a vehicle on a long trip, the EV requires a battery subject to drawbacks such as heavy weight, long charging time, and large size. In conjunction with these obstacles, EVs have a relatively short driving range compared to their petroleum powered counterparts. To be adopted widely, EVs need to overcome these drawbacks. To alleviate the battery-related problems, wireless power transfer (WPT) systems have been developed and successfully deployed at various public sites to charge Online EVs (OLEVs) while they are moving [7, 8]. To increase vehicle driving range, the WPT charges OLEVs in-motion, when they pass charging sections installed in roads, without physical contact between the utility power supply and vehicle battery. Several works study the impact stationary charging of EVs has on the power grid during different periods of day [9–11]. However, the integration of OLEVs into the power grid would increase the unpredictable load and congestion of the power system operator [12]. In addition, power system operators use *ancillary services* to maintain the stability between power supply and demand to secure reliable functionality of the power supply and ancillary services require a quick response from the power resources. Thus, the integration of OLEVs into the power grid would also increase the ancillary services cost of the grid operators.

It is very important to avoid congestion and balance load at different points of the grid so that the power grid operator can provide quality of service (QoS) and encourage OLEVs to get energy from the power grid while they are running on the road. There should be some policies to balance the load and avoid congestion at different points of the power grid [13–16]. Previous works (e.g., [17, 18, 9–11, 19]) do not proactively disincentivize OLEVs from power allocation when the power usage is high at charging sections.

In this paper, we consider a WPT system where several charging sections are installed on top of a road or charging lane. As a control unit of the power grid, the smart grid is capable of processing data and communicating with others. The smart grid is connected with the charging sections. While driving, OLEVs can get energy from the smart grid via the charging sections. In rest of the paper, we use the term "power" as the transfer rate of energy. Fig. 1 shows an example of a WPT system architecture. Each OLEV can communicate
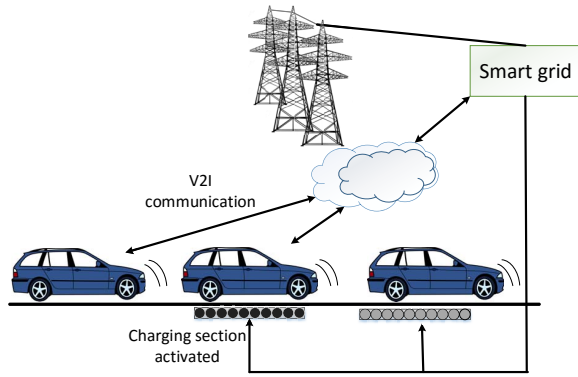
IEEE
computer
society

Fig. 1: The wireless power transfer system.

with the smart grid using vehicle-to-infrastructure (V2I) communication. An OLEV may spend very little time on top of a charging section based on its driving velocity. When approaching a charging lane, the OLEVs and the smart grid can share information with each other to find out the time each OLEV would spend on top of charging sections. However, more than the expected number of OLEVs at a charging section at the same time easily leads to overload at the charging section. As OLEVs do not know the expected amount of power capacity of each charging section to avoid congestion at the charging sections, the smart grid should determine some policies to avoid congestion at the charging sections to ensure the QoS to the OLEVs.

In this paper, at first, we conduct a study to show the existence of unpredictable power load and congestion because of OLEVs. We use daily traffic counts (the number of vehicles) in the *New York City* (NYC) [20] and the *Simulation for Urban MObility* (SUMO) tool to predict the amount of power OLEVs can receive over the course of the day depending on the number of OLEVs and their onboard energy.

We aim to maximize the social welfare of the OLEVs that are in the WPT system. We define the social welfare of OLEVs as a function which jointly considers the total satisfaction of the OLEVs and the power charging cost over all the charging sections. We introduce the power charging cost to take into consideration of power demand, energy transfer efficiency, and power capacity at each charging section. To maximize the social welfare of OLEVs, we propose a nonlinear pricing policy to determine the power payment function for OLEVs, which decentivizes OLEVs proactively to request more power when the power usage is high. Next, we design a strategy game between different OLEVs with the help of smart grid to find the optimal power schedule for OLEVs that maximizes the social welfare of OLEVs. Based on the satisfaction function and power payment function of OLEVs, we use the proposed game to find the socially optimal power schedule. To find the socially optimal power schedule, we use a decentralized framework which involves iterative interaction among the OLEVs and the smart grid. In the framework, we use an asynchronous strategy where the OLEVs update their power

request according to the updated power payment function that is calculated by the smart grid. We mathematically prove that the best response strategy of the OLEVs converges to an unique socially optimal power schedule. Finally, we evaluate our nonlinear pricing policy in the simulation study.

The rest of this paper is organized as follows: Section II presents an overview of related work. Section III presents the background and motivation behind this work. Section IV presents the problem formulation and game theory-based distributed pricing policy for power transfer from the charging sections to OLEVs to find out the optimal power schedule using best response strategy. Section V presents a simulation study to verify the performance of our proposed pricing mechanism. Finally, Section VI concludes this paper with remarks on our future work.

II. RELATED WORK

As a part of the future generation intelligent transportation systems [21–26], design criteria of the WPT systems is discussed thoroughly in several existing works [27–32]. The studies [27, 29] present different kinds of EV components and the research challenges associated with the WPT systems. Onar *et al.* presented an overview of WPT magnetic field measurements with discussion of several factors in the power transfer procedures with the consideration of highway surfacing materials [28]. Li *et al.* thoroughly presented an analytic study of the technologies in the area applicable to EV wireless charging [30]. The work [32] presents the design of the electric components, an electromotive force shielding, and an optimized core structure with large air gaps for the WPT systems. The work [7] presents a WPT system consisting of a cloud-based global grid controller and a fog-based local grid controller and the authors tried to balance the SOC of OLEVs considering several factors, i.e., different numbers of OLEVs with heterogeneous vehicle parameters and priorities, different sources-destinations, available energy, etc using gradient based optimization method. The study by Ko and Jang [33] focuses two main factors for a WPT system: the battery size and the positions of power transmitters on the road. The authors presented the solution of an optimization model using particle swamp optimization technique to minimize the infrastructure cost with reference to the battery size, the total number of power transmitters, and their allocation. Another study [12] presents a novel bidirectional WPT system for EV and V2G systems which includes loose magnetic coupling charging and discharging procedures. However, these methods do not consider economical benefit of the WPT systems where the smart grid can share its energy with OLEVs while they are running.

Another set of existing works analyze the impact of stationary charging of EVs on the power grid [9–11, 18]. Chen et. al [11] proposed research challenges to introducing the integration of EVs into the power grid systems; especially, they considered the existing load fluctuations of the power grid and how these fluctuations would impact the integration of EVs.

The authors [10] presented an optimization framework to maximize the profit of EVs and satisfy trip energy requirements with the consideration of bi-directional charging infrastructure. To reduce the ancillary services cost and provide more flexibility, the work [9] proposes a mathematical model to share surplus energy from vehicles to the power grid. Tushar et. al [17] presented a noncooperative Stackelberg game to facilitate the energy trading between plug-in EVs and the smart grid. In this game the smart grid would maximize its revenue whereas plug-in EVs would balance the tradeoff between the battery charging and its associated costs. However, the capacity of the power grid operator and congestion degree should be considered to reduce the operating cost of the power grid. In this paper, we introduce a game theory-based pricing policy [34] to incentivize the power grid when the congestion degree is high.

III. BACKGROUND AND MOTIVATION

In this section, we try to verify the existence of power deficiency in a grid where the smart grid shares its energy with OLEVs using the WPT systems. At first, we look at the power load of an existing grid operator to check if there is any power deficiency such that congestion exists. Here, by the word "congestion", we mean that the demand from OLEVs is larger than the power supply capacity at charging sections due to the power deficiency. Then, we try to figure out the approximate amount of energy OLEVs can receive in a single day based on the real traffic trace of road sections.

Usually, electricity provided by the grid is grouped in several different markets with correspondingly different control periods. In electricity networks, there are four control periods: baseload power, peak power, spinning reserves, and frequency control. These control periods mainly differ in electricity control method, response time, duration of the power dispatch, contract terms, and price [35]. Baseload power is provided by large power plants. Next, peak power is required at times of day when power requirements are high. Then, spinning reserve refers to the situation when power is needed immediately. Finally, frequency control power is used to calibrate the frequency and voltage of the grid by matching generation to load demand. Usually, spinning reserves and frequency control are forms of electric power referred to as "ancillary services". The demand of a power grid varies based on its customer types, coverage area, time of day, day of week, and so on. According to the *New York Independent System Operator* (NYISO), the power demands are different in different regions so that the electricity prices are varied based on the regional demand and regional capacity and the operator needs to pay some extra money due to power deficiency [36]. In addition to ancillary services are services to ensure incessant power supply which cost about 5–10% of total electricity cost, which is about $12 billion per year in the U.S. [35]. The existence of power deficiency would be a consequence of spending more money for running ancillary services. As a matter of fact, the interaction between the power grid and EVs offers possibilities of more deficiency for the power grid system.
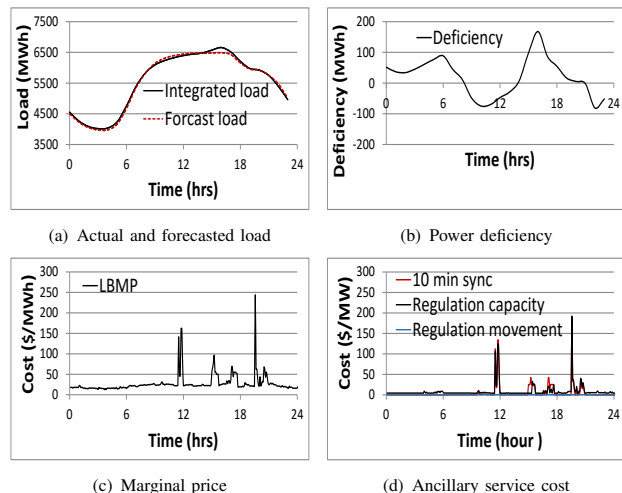

(a) Actual and forecasted load   (b) Power deficiency

(c) Marginal price   (d) Ancillary service cost

Fig. 2: Power grid data from NYISO [36].

To verify the amount of existing power deficiency, we collect and process NYISO's load, price, and ancillary services data of 12 May 2016. Fig. 2(a) shows load information on 12 May 2016 where we can find that power load varied from 4017.1MWh to 6657.8MWh for the day. Fig. 2(b) shows the power deficiency (the difference between integrated load and forecast load) for the same day where the deficiency would be as high as 167.8MWh. In this instance, integrated load is actual load generated by regular consumers of NYISO on that day and forecast load is the predicted load by NYISO. The power deficiency is basically caused by the uncertain nature of regional power demand. Fig. 2(c) shows how much the location-based marginal price (LBMP) varied throughout the day due to the power deficiency. LBMP is decided based on regional power demand and regional power supply [36]. In such a case, LBMP would be as low as $12.52 to as high as $244.04 based on the power deficiency. And, Fig. 2(d) shows how much NYISO needs to pay for ancillary services on the same day which varies based on the current power demand; on average NYISO pays $13.41 on 12th May 2016. Based on the above discussion, we can easily state that in the existing power grid, power deficiency exists due to the unpredictable load variations and the integration of OLEVs in the smart grid would create more unpredictable load and increase the power deficiency.

Now, we try to show that WPT systems can cause unpredictable power load and the integration of OLEVs in the power grid would create congestion at charging sections. We present a real traffic trace-based simulation study to predict the amount of energy OLEVs can receive from the power grid using WPT system. To motivate our work, we illustrate the potential deficiency caused by WPT systems to the smart grid of a city. The amount of energy received by OLEVs depends on the intersection time between OLEVs and charging sections. Here, the intersection time is the actual time OLEVs spend on top of the charging sections. This intersection time actually depends on charging section coverage, charging sec-
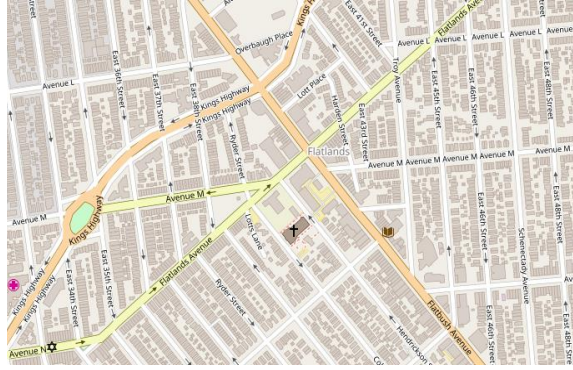
(a) OpenStreetMap
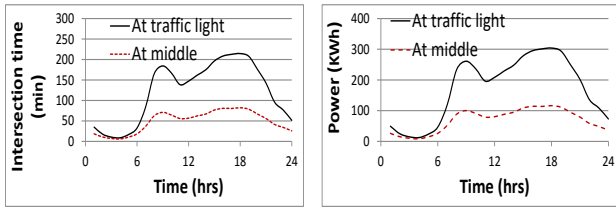
(b) Intersection time

(c) Amount of Power

Fig. 3: Simulated intersection time and amount of power between OLEVs and charging sections on *Flatlands Avenue in Brooklyn, NYC* on January 31, 2013.

tion placement, OLEV participation, and OLEV willingness, which are defined as followings: *Charging section coverage* is the total length of installed charging sections and it mainly includes the consideration of initial investment; *Charging section placement* is simply the location of the charging sections; *OLEV participation* is the fraction of total vehicles equipped as OLEVs; and *OLEV willingness* is the fraction of OLEVs that are both willing and able to get energy from the smart grid. Of these factors, placement is the least quantifiable. Typically, placement in various congested traffic areas will increase intersection time. The other factors of coverage, participation, and willingness are positively correlated with intersection time. We expect more coverage and participation to increase in cities as the benefits of the WPT systems become pronounced. Willingness can be maximized by a fair pricing system that incentivizes the smart grid to sell their energy, as proposed in this paper.

We conduct the study based on the available traffic count of the *NYC* from *New York City Department of Transportation* (NYCDOT) on January 31st, 2013 [20]. Here, we use the SUMO to generate the traffic based on the hourly traffic counts. We set state of charge (SOC) of each vehicle's battery is equal to 50% and the maximum capacity of vehicle's battery is 2,000KWh. Here, SOC represents the amount of energy stored in the battery at a certain time. We first download the Flatlands Avenue in Brooklyn map from OpenStreetMap to use with SUMO (as shown in Fig. 3(a)). In SUMO, vehicles follow a car following model, maintain the inter-vehicle safety distances [37] and follow the speed limits of the road network. For a 200 total meters of charging section

having 100KW capacity placed around an intersection, our simulation predicts a total of over 48 hours of intersection time between vehicles and charging section over the course of 24 hours. The total intersection time considers the average time of all vehicles on top of charging section (i.e., 100 vehicles and 2 minutes average time on charging section result in approximately 3 hours total intersection time). The hourly intersection is depicted in Fig. 3(b), as traffic changes throughout the day. The upper solid line has the charging section placed immediately before the traffic lights, and the dashed line shows the intersection time if the charging section is placed at the middle of a road instead. Fig. 3(c) shows the projected power from the grid if we consider full participation based on previous Fig. 3(b). Here, participation is the fraction of total vehicles equipped as OLEVs. We find that OLEVs can get as much as 4146.16KWh power from this intersection. As of June 2011, there were 4371 intersections with traffic lights in Brooklyn[1]. If we consider some other intersections in NYC, then the aggregated power amount will be enough to increase the power demand of the grid operator. Based on OLEV participation and OLEV willingness, the power demand would not be fixed over the period of time and the demand would also be varied for different regions at same time. From the above discussion, we can conclude that the load caused by OLEVs in the power grid is not easily predictable and the number of OLEVs would cause congestion at different charging sections throughout the day.

IV. GAME THEORY-BASED PRICING FOR WIRELESS POWER TRANSFER SYSTEM

In this section, we present a brief introduction of WPT system in Sub-Section IV-A. Then, we formulate the problem to find the optimal power schedule to transfer power from charging sections to OLEVs and avoid congestion at charging sections. To achieve this objective, the smart grid specifies a nonlinear pricing policy that has a higher unit price when the current energy sharing is higher comparing with the current demand.

A. Wireless Power Transfer System

Suppose, several OLEVs are running on a lane. Each OLEV is equipped with a battery to carry out the energy for the entire travel time. The SOC of battery represents the amount of energy stored at a particular time. During the trip, it might be necessary that OLEVs need to take energy from the smart grid. To facilitate the energy transportation, there are several charging sections installed on top of the lane. The charging sections are connected with the smart grid. In our model, we consider a charging infrastructure where the smart grid can transfer energy to OLEVs without having any physical contacts. During the peak hours, the power load of smart grid is varied and the integration of OLEVs into smart grid causes a tremendous amount of unanticipated energy demand, and, hence causes congestion at different charging sections.

[1]www.nyc.gov/html/dot/html/infrastructure/signals.shtml

Based on the expected travel time, each OLEV can decide the amount of SOC it needs to finish the trip. Before approaching to the charging lane, OLEVs can communicate with the smart grid to inform their current positions and velocities. On the other hand, the smart grid notifies OLEVs about the number of charging sections and their positions. In this way, both OLEVs and the smart grid can calculate the expected travel time to reach different charging sections. The communication between OLEVs and the smart grid can be taken place by V2I communication (i.e., using IEEE-802.11p or 4G-LTE enabled devices).

In our WPT system, several factors limit the amount of power distribution from smart grid to OLEVs. First, the capacity of the power line of each charging section and the total time OLEVs stay on top of the charging sections are the upper limits that each OLEV can receive the power to grid. Here, the capacity of power line of a charging section can be represented as follows [38]:

$$P_{\text{line}} = \frac{V \cdot Curr \cdot l}{vel}. \tag{1}$$

Here, V is the line voltage, $Curr$ is the maximum rated current, l is the charging section length and vel is the velocity of the OLEV. Since the line voltage, maximum current rate and charging section length are almost fixed values for different OLEVs, the P_{line} only depends on the velocity of OLEVs.

Next, the approximate amount of energy an OLEV can receive is also limited by the required energy to finish its trip minus the energy stored inside the battery. Basically, it is the energy needed for planned travel minus the onboard energy storage times the efficiency of converting stored energy to grid power, then all divided by the duration of time the energy is dispatched. It means [38]:

$$P_n^{\text{OLEV}} = \frac{(SOC_n^{\text{req}} - SOC_n + SOC_{\text{min}}) \cdot P_{\text{max}} \cdot \eta_E}{\eta_{OLEV}}, \tag{2}$$

where P_{max} is maximum power of the battery of OLEV in kW, SOC_{min} is the minimum value of SOC, SOC_n^{req} is the required SOC to finish OLEV n's trip, η_{OLEV} is the vehicle driving efficiency, η_E is energy transfer efficiency. Here, SOC_n and SOC_n^{req} are decreasing over the distance OLEV traveled so far and thus, P_n^{OLEV} is varied based on the time and OLEV's properties. Thus, the total amount of power an OLEV can receive is actually limited by:

$$p_{\text{n,c}} \leq min(P_{\text{line}}, P_{\text{OLEV}}). \tag{3}$$

Here, $p_{\text{n,c}}$ is amount of power an OLEV n can receive from a particular charging section c.

In next Sub-Section, we introduce the problem to find out the optimum pricing policy of the smart grid.

B. Problem Statement

Suppose, there is a set $\mathcal{N}$ of OLEVs into our WPT system where $\mathcal{N} = \{1, 2, ..., N\}$ and there is a set $\mathcal{C}$ of charging sections installed on top of the charging lane where $\mathcal{C} = \{1, 2, ..., C\}$ (as Fig. 4 shows). Let us denote $p_{n,c}$ the
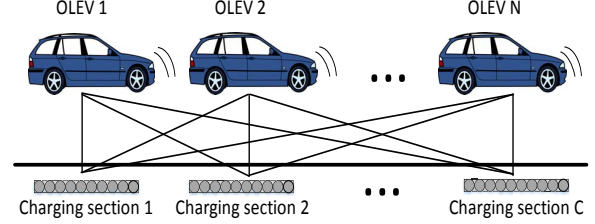

Fig. 4: The mapping between OLEVs and charging sections.

amount of power OLEV n can get from charging section c at a particular time. For a charging section c, $P_c = \sum_{n \in \mathcal{N}} p_{n,c}$ as the total power provided to all available OLEVs. We denote $\frac{P_c}{P_{line}}$ as the congestion degree of charging section c. Let us consider $p_n = \sum_{c \in \mathcal{C}} p_{n,c}$ as the total amount of power allocated to OLEV n using all available charging sections and $\mathbf{p}_n = (p_{n,1}, ..., p_{n,C})$ as the power schedule for OLEV n from all charging sections. We define the power schedule for the OLEVs in the system as $\mathbf{p} = (\mathbf{p}_1, ..., \mathbf{p}_N)$ and we also define the charging schedule for all the OLEVs except OLEV n as $\mathbf{p}_{-n}$. Since an OLEV cannot accept more than its capacity P_n^{OLEV}, $p_n \leq P_n^{OLEV}$ always satisfies. We consider $\mathcal{P}_n = \{\mathbf{p}_n | \sum_{c \in \mathcal{C}} p_{n,c} \leq P_n^{OLEV}\}$ as the set of all feasible power distribution schedule of OLEV n, and we define $\mathcal{P} = \mathcal{P}_1 \times ... \times \mathcal{P}_N$ as the set of all feasible power schedule for all OLEVs. Since $\mathcal{P}$ is a compact and convex set, the power schedule must satisfy each charging section's capacity constraint:

$$P_{\text{c}} = \sum_{n \in \mathcal{N}} p_{\text{n,c}} \leq \eta P_{\text{line}}, \tag{4}$$

where $\eta \in [0, 1]$ is the safety factor determined by the smart grid to ensure that maximum capacity is not violated.

Next, we formulate the social welfare and utility functions of OLEVs. We consider $\mathcal{U}_n(\sum_{c \in \mathcal{C}} p_{n,c})$ as the satisfaction function of OLEV n for power schedule $\mathbf{p}_n$. Since a higher power arrangement makes an OLEV more satisfied, the satisfaction function $\mathcal{U}_n(\cdot)$, is considered to be non-decreasing. However, the level of satisfaction of OLEV gradually gets saturated based on the current SOC of the battery. Thus, we can consider, $\mathcal{U}_n(\cdot)$ is a strictly increasing and strictly concave, and its second derivative is continuous in $\mathbf{p}_n$. We represent $\mathcal{V}(P_c)$ as the power charging cost for getting P_c of power from charging section c. Thus, we can define *social welfare* of OLEVs as satisfaction of OLEVs minus the cost related to the amount of power charging:

$$\mathcal{W}(\mathbf{p}) = \sum_{n=1}^{N} \mathcal{U}_n(\sum_{c \in \mathcal{C}} p_{n,c}) - \sum_{c \in \mathcal{C}} (\mathcal{V}(P_c))$$
$$\text{s.t.} \quad P_c - \eta P_{line} \leq 0, \quad \forall c.$$
$$\mathbf{p} \in \mathcal{P}. \tag{5}$$

To integrate the constraints in the Equation (5) as in [39], we change Equation (5) to an objective function such that the power schedule maximizes the social welfare. We define

1201

$A(\cdot)$ as the overload cost function associated with a charging section. We define $\mathcal{Z}(x) \doteq \mathcal{V}(x) + A(x - \eta P_{line})$ as the power charging cost, and overload cost for power reservation x from a charging section. As $\mathcal{V}(\cdot)$ and $A(\cdot)$ are strictly convex functions, $\mathcal{Z}(\cdot)$ is also strictly convex function. Since $\mathcal{U}_n(\cdot)$ is strictly concave for each OLEV n and $\mathcal{Z}(\cdot)$ is strictly convex, $\mathcal{W}(\cdot)$ is a strictly concave function in $\mathcal{P}$. Thus, we can redefine social welfare of OLEVs from Equation (5) as follows:

$$\mathcal{W}(\mathbf{p}) = \sum_{n=1}^{N} \mathcal{U}_n(\sum_{c \in C} p_{n,c}) - \sum_{c \in C} \mathcal{V}(P_c) \qquad (6)$$

$$- \sum_{c \in C} A(P_c - \eta P_{line}) \doteq \sum_{n=1}^{N} \mathcal{U}_n(p_n) - \sum_{c \in C} \mathcal{Z}(P_c),$$
$$\mathbf{p} \in \mathcal{P}. \qquad (7)$$

In Equation (7), we consider the socially optimal power schedule as a feasible power schedule which maximizes the social welfare of OLEVs. The smart grid determines the payment for all OLEVs based on the capacity and currently available power from charging sections.

In next Sub-Section, we introduce smart grid's pricing policy for individual OLEV.

C. Pricing Policy

In this Sub-Section, we propose the power pricing policy for OLEVs. Notice that this policy helps to avoid congestion and it also provides load balancing among charging sections. The smart grid transfers the power charging cost from charging sections to OLEVs. Let us define $\mathcal{Y}_{n,c}(\mathbf{p})$ as the power charging cost where OLEV n has been scheduled $p_{n,c}$ power schedule and the other OLEVs have been scheduled $\mathbf{p}_{-n}$ power schedule on charging section c:

$$\mathcal{Y}_{n,c}(\mathbf{p}_{-n}, p_{n,c}) = \mathcal{Z}\left(\sum_{j \in \mathcal{N}/\{n\}} p_{j,c} + p_{n,c}\right). \qquad (8)$$

To pay for power schedule $\mathbf{p}_n$ of OLEV n from charging sections, we formulate the power payment function as $\xi_n(\mathbf{p}_{-n}, \mathbf{p}_n)$ based on the fixed cost function as in the following:

$$\xi_n(\mathbf{p}_{-n}, \mathbf{p}_n) = \sum_{c \in C} [\mathcal{Y}_{n,c}(\mathbf{p}_{-n}, \mathbf{p}_n) - \mathcal{Y}_{n,c}(\mathbf{p}_{-n}, \mathbf{0})]. \qquad (9)$$

For each OLEV, Equation (9) is unbiased cost function, i.e., $\xi_n(\mathbf{p}_{-n}, \mathbf{0}) = 0, \forall n$, due to the fact that the term $\mathcal{Y}_{n,c}(\mathbf{p}_{-n}, \mathbf{0})$ is independent from $\mathbf{p}_n$. It means that if OLEV n does not get any power from chargingsections, it does not need to pay anything.

Actually, OLEV n pays based on its allocated power p_n and scheduled power $\mathbf{p}_n$ over all chargingsections. Let us denote:

$$\mathcal{P}_n(p_n) = \{\mathbf{p}_n | \sum_{c \in C} p_{n,c} = p_n, \forall C \in \mathcal{N} : p_{n,c} \geq 0\}, \qquad (10)$$

as the set of all feasible power schedules that OLEV n can choose to schedule power from charging sections when OLEV n requests p_n amount of power to the smart grid. Now, OLEV

n's power schedule $\mathbf{p}_n$ is selected from all the feasible power schedules as the amount of power to be transferred from charging sections. Actually, the smart grid selects the power schedule $\hat{\mathbf{p}}_n(p_n)$ to minimize the cost from chargingsections. Also, the selected power schedule minimizes the payment for OLEV n:

$$\hat{\mathbf{p}}_n(p_n) = \arg \min_{\mathbf{p}_n \in \mathcal{P}_n(p_n)} \sum_{c \in C} \mathcal{Y}_{n,c}(\mathbf{p}_{-n}, p_{n,c})$$
$$= \arg \min_{\mathbf{p}_n \in \mathcal{P}_n(p_n)} \xi_n(\mathbf{p}_{-n}, \mathbf{p}_n). \qquad (11)$$

We represent $\hat{p}_{n,c}(p_n)$ as c^{th} component of the feasible power schedule $\hat{\mathbf{p}}_n(p_n)$, which is derived from Equation (11). Now, we define $[x]^+ = \min\{0.x\}$. In the following, Lemma IV.1 shows the processes to find out the unique power schedule $\hat{\mathbf{p}}_n(p_n)$ for OLEV n by the smart grid.

Lemma IV.1. *There exists a unique constant level $\lambda^*(p_n)$ in the total allocated power p_n of OLEV n so that $\hat{\mathbf{p}}_n(p_n)$ is uniquely evaluated as in the following:*

$$\hat{p}_{n,c}(p_n) = [\lambda^*(p_n) - \sum_{j \in \mathcal{N}/\{n\}} p_{j,c}]^+, \forall c \in \mathcal{C}. \qquad (12)$$

Proof. We define $\mathcal{L}(\mathbf{p})$ as the Lagrangian of the objective function of the term $\xi_n(\mathbf{p}_{-n}, \mathbf{p}_n)$ from Equation (11) as in the following:

$$\mathcal{L}(\mathbf{p}_{-n}, \mathbf{p}_n) = \xi_n(\mathbf{p}_{-n}, \mathbf{p}_n) - \rho\left(\sum_{c \in C} p_{n,c} - p_n\right). \qquad (13)$$

Here, ρ is the Lagrange multiplier for the above equation. $\hat{\mathbf{p}}_n(p_n) \in P_n(p_n)$ minimizes $\xi_n(\mathbf{p}_{-n}, \mathbf{p}_n)$ in $\mathcal{P}_n(p_n)$. Using the Karush–Kuhn–Tucker (KKT) necessary conditions as in Proposition 3.3.1 in [39], we can state that there is a constant ρ^* such that for every c in $\mathcal{C}$, we have:

$$\nabla_c \mathcal{L}(\mathbf{p}_{-n}, \hat{\mathbf{p}}_n) = \mathcal{Z}'\left(\sum_{j \in \mathcal{N}/\{n\}} p_{j,c} + \check{p}_{n,c}(p_n)\right) \qquad (14)$$
$$- \rho^* = 0.$$

Since $\mathcal{Z}$ is a strictly convex function, its first order derivative $\mathcal{Z}'$ is a strictly increasing function. Thus, $\mathcal{Z}'$ is a one-to-one function, and its inverse function $(\mathcal{Z}')^{-1}$ exists. We define $\lambda^*(p_n) = (\mathcal{Z}')^{-1}(\rho^*)$. From Equation (14), we can derive:

$$\lambda^*(p_n) = (\mathcal{Z}')^{-1}(p^*) = \sum_{j \in \mathcal{N}/\{n\}} p_{j,c} + \hat{p}_{n,c}(p_n), \forall c \in \mathcal{C}. \quad (15)$$

The results in Equation (12) directly follows Equation (15) due to the fact that $\check{p}_{n,c}(p_n) \geq 0$. $\square$

The smart grid tries to minimize power charging cost for chargingsections and it calculates the power payment function based on power schedule $\hat{\mathbf{p}}_n(p_n)$. Then, the smart grid proposes payment function $\Psi_n(p_n)$ to OLEV n, for p_n amount of power from charging sections as follows:

$$\Psi_n(p_n) = \xi_n(\mathbf{p}_{-n}, \hat{\mathbf{p}}_n(p_n)). \qquad (16)$$

1202

Then, to get p_n amount of power, the utility function of OLEV n is denoted as $\mathcal{F}_n(p_n, \Psi_n(\cdot))$ and it is calculated as follows:

$$\mathcal{F}_n(p_n, \Psi_n(\cdot)) = \mathcal{U}_n(p_n) - \Psi_n(p_n), \qquad (17)$$

$\Psi_n(\cdot)$ is derived from the initial power schedule of all OLEVs except OLEV n (denoted as $\mathbf{p}_{-n}$) and the requested power schedule for OLEV n (denoted as $\hat{\mathbf{p}}_n(p_n)$). We can also define the utility function as $\mathcal{F}_n(\mathbf{p}_{-n}, \mathbf{p}_n)$:

$$\mathcal{F}_n(\mathbf{p}_{-n}, \mathbf{p}_n) = \mathcal{U}_n\left(\sum_{c \in \mathcal{C}} p_{n,c}\right) - \xi_n(\mathbf{p}_{-n}, \mathbf{p}_n). \qquad (18)$$

In following, Lemma IV.2 shows that chosen power schedule by the smart grid for an OLEV is the best strategy to minimize the power charging cost over the chargingsections.

Lemma IV.2. *From Equation (16), when the power schedule of other OLEVs is $\mathbf{p}_{-n}$, the smart grid proposes power payment function $\Psi_n(\cdot)$ for OLEV n. The total received power to maximize the utility of OLEV n, p_n^*, is unique based on Equation (17). From Equation (11), the unique power schedule $\mathbf{p}_n^* = \hat{\mathbf{p}}_n(p_n^*)$ is derived and it maximizes the utility function of charging section n, $\mathcal{F}_n(\mathbf{p}_{-n}, \mathbf{p}_n)$ based on Equation (18).*

Proof. $\Psi_n(\cdot)$ is a strictly convex function in $[0, P_n^{OLEV}]$ and $\mathcal{U}_n(\cdot)$ is a strictly concave function in $[0, P_n^{OLEV}]$. Thus, the utility function $\mathcal{F}_n(p_n, \Psi_n(p_n))$ is a strictly concave function in p_n. To maximize $\mathcal{F}_n(p_n, \Psi_n(p_n))$ in $[0, P_n^{OLEV}]$, p_n^* is the unique total amount of power. Thus, using Lemma IV.1, the power schedule $\hat{\mathbf{p}}_k(p_n^*)$ is the unique power schedule to minimize $\xi_n(\mathbf{p}_{-n}, \mathbf{p}_n)$ in $\mathcal{P}_n(p_n^*)$. It implies that $\hat{\mathbf{p}}_n(p_n^*)$ is the unique power schedule to minimize $\mathcal{F}_n(\mathbf{p}_{-n}, \mathbf{p}_n)$ in $\mathcal{P}_n$, if and only if:

$$p_n^* = \arg\max_{p_n \in [0, P_n^{OLEV}]} \mathcal{F}_n(p_n, \Psi_n(\cdot)$$
$$\Leftrightarrow \hat{\mathbf{p}}_n(p_n^*) = \arg\max_{\mathbf{p}_n \in \mathcal{P}_n} \mathcal{F}_n(\mathbf{p}_{-n}, \mathbf{p}_n). \qquad (19)$$

$\square$

We assume that OLEVs' satisfaction functions are unknown to the smart grid. The demand of each OLEV would be different than other OLEVs. Thus, it is reasonable to assume that the smart grid asks OLEVs for power requirements and based on the price function, each OLEV wants to maximize their own utility and requests power amount to the smart grid. Our main goal is to maximize social welfare of OLEVs. It motivates us to design a strategic game between OLEVs which is managed by the smart grid. In this game, the smart grid gathers all the power requirements of the OLEVs, and then proposes the power payment function $\psi_n(\cdot)$ for each OLEV n. Then, each OLEV n receives the response from the smart grid and decides the total power p_n for itself (OLEV n) to maximize their own utility. Then, based on OLEV n's total power p_n, the smart grid determines the power schedule $\mathbf{p}_n(p_n)$ and power payment function $\psi_n(\cdot)$ again. Actually, the smart grid recalculates the power payment functions to minimize the cost and notifies to OLEVs again.

As we mention earlier, the smart grid does not know the satisfaction functions of the OLEVs. Then, we need an iterative decentralized optimization framework to find the socially optimal power schedule. In the next subsection, we propose a distributed optimization update process to find out the socially optimal power schedule.

D. Asynchronous-based Best Response Strategy

In this Sub-Section, we present distributed updating process to find the socially optimal power schedule. In proposed decentralized framework, it is not necessary to reveal satisfaction function $\mathcal{U}_n(\cdot)$ of OLEVs to the smart grid. The smart grid uses an asynchronous-based best response strategy to decide the power for each OLEV as in [40].

1) Decentralized Power Schedule: In a decentralized updating framework, the best response strategy for each OLEV is performed in the step-by-step iterative process. At first, the smart grid reports the power payment function $\Psi_n(.)$ to each OLEV n to minimize the power charging cost over charging sections in every step based on Lemma IV.1.

Then, a randomly chosen OLEV n updates its power request to maximize its utility function $\mathcal{F}_n(p_n, \Psi_n(.))$. Based on the response from OLEV n, the smart grid finds the power schedule that minimizes power charging cost over the all charging sections as in Lemma IV.1 and updates the power payment function $\Psi_n(.)$ again and charging section's utility $\mathcal{F}_c(p_c, \Psi_c(.))$ to OLEVs. Then, OLEVs updated their power deduction amount and notify the smart grid. The smart grid finds the power schedule that minimizes OLEVs' power deduction cost over the all charging sections as in Lemma IV.1. At iteration step k, we use $\mathbf{p}^k$ as the updated power schedules of OLEVs. The smart grid updates the power payment function of OLEV n at step $k + 1$, $\Psi_n^{k+1}(\cdot)\forall n \in \mathcal{N}$ as follows:

$$\Psi_n^{k+1}(p_n) = \xi_n(\mathbf{p}_n^k, \hat{\mathbf{p}}_n(p_n)), \forall n. \qquad (20)$$

Next, the smart grid announces the new power payment function $\Psi_n^{k+1}(.)$ and new power schedule p_n^{k+1} to OLEV n. Each OLEV n tries to maximize its individual utility based on the response from the smart grid as follows:

$$p_n^{k+1} = \arg\max_{p_n \in \mathcal{P}_n} \mathcal{F}_n(p_n, \Psi_n^{k+1}(\cdot))$$
$$= \arg\max_{p_n \in \mathcal{P}_n} \mathcal{U}_n(p_n) - \Psi_n^{k+1}(p_n). \qquad (21)$$

Then, OLEV n notifies the newly calculated power amount (based on its maximized utility) to the smart grid.

In the next subsection, we discuss the best response strategy for each OLEV on how to find the the amount of power request to maximize its utility.

E. Best Response Updating Strategy For an OLEV

In the proposed best response updating process, Equation (21) is used to find the optimal power request for an OLEV at step $k + 1$. The optimal power request is derived as in the following Lemma.

Lemma IV.3. *The optimal power request for an OLEV n at $(k + 1)^{th}$ update iteration is derived as in the following:*

1203

$$p_n^{k+1} = \begin{cases} 0, & \frac{\delta \mathcal{F}_n}{\delta p_n}(p_n, \Psi_n(p_n)) < 0, \\ P_n^{OLEV}, & \frac{\delta \mathcal{F}_n}{\delta p_n}\left(P_n^{OLEV}, \psi_n(P_n^{OLEV})\right) > 0, \\ \arg_{p_n \in [0, P_n^{OLEV}]}\left\{\frac{\partial \mathcal{F}_n}{\partial p_n}(p_n, \psi_n(p_n)) = 0\right\}, otherwise \end{cases}$$

(22)

Proof. The proof follows from the strictly concavity of $\mathcal{F}_n(p_n, \Psi_n(p_n))$ in $[0, P_n^{OLEV}]$ with applying the first order inequality condition as in [39]:

$$\frac{\delta \mathcal{F}_n}{\delta p_n}(p_n, \Psi_n(p_n))(p_n - p_n^{k+1}) \leq 0, \forall p_n \in [0, P_n^{OLEV}]. \quad (23)$$

for three possible cases: (i) $\frac{\delta \mathcal{F}_n}{\delta p_n}(p_n, \Psi_n(p_n)) < 0$, (ii) $\frac{\delta \mathcal{F}_n}{\delta p_n}(p_n, \Psi_n(p_n)) > 0$, (iii) $\frac{\delta \mathcal{F}_n}{\delta p_n}(p_n, \Psi_n(p_n)) \leq 0$ and $\frac{\delta \mathcal{F}_n}{\delta p_n}(p_n, \Psi_n(p_n)) \geq 0$. For these three possible cases, the unique solution to Equation (21) that maximizes the utility of OLEV n at $(k+1)^{th}$ update step is derived as in Equation (22). $\square$

F. Power Schedules of Charging Sections

Based on the iterative updating process, the smart grid determines the power schedule for the OLEVs over all the charging sections. The smart grid finds the unique constant value $\lambda^*(p_n^{k+1})$ to determine the power schedule $(\mathbf{p}_n^{k+1} = \hat{\mathbf{p}}_n(p_n^{k+1}))$ for OLEV n as in Equation (12). We define the function $Y(x), x \in \mathbb{R}$, as in the following:

$$Y(x) = \sum_c \left[x - \sum_{j \in \mathcal{N}/\{n\}} p_{j,c}\right]^+, x \in \mathbb{R}. \quad (24)$$

$Y(x)$ is a strictly increasing function of x, $(x \in \mathbb{R})$ and the function $Y(x) - a = 0$ has a unique solution for $a \geq 0$. We get $Y(\lambda^*(p_n)) = \sum_c p_{n,c} = p_n$ from Equation (12). The unique root of the function $Y(x) - p_n^{k+1} = 0$, is equal to $\lambda^*(p_n^{k+1})$. To find out $\lambda^*(p_n^{k+1})$, the smart grid can use the bisection method as $p_n^{k+1} \geq 0$. Eventually, the smart grid finds the power schedule for OLEV n at charging sections based on Equation (12).

G. Convergence Analysis

In this subsection, we show that the proposed best response updating strategy converges to a socially optimal power schedule.

Theorem IV.1. *The best response update process converges to a socially optimal power schedule.*

Proof. Now, we show that $\mathbf{p}^*$ maximizes $\mathcal{W}(\mathbf{p})$ over $\mathcal{P}$. Let us show that $\mathbf{p}^{k_i+1} - \mathbf{p}^{k_i}$ converges to zero. Assume the contrary, i.e. $\mathbf{p}^{k_i+1} - \mathbf{p}^{k_i}$ does not converge to zero. We consider $\delta^{k_i} = \| \mathbf{p}^{k_i+1} - \mathbf{p}^{k_i} \|_2$. There exists a subsequence $\{l_i\} \subseteq \{k_i\}$ and $\exists \delta_0 > 0$ such that $\delta^{l_i} > \delta_0$ based on our contrary non-convergence assumption. Since the length of the sequence $\{l_i\}$ is infinite and the set $\mathcal{N}$ is finite and fixed, the power schedule $\mathbf{p}_n$ of OLEV $n \in \mathcal{N}$ is updated in an infinite length subsequence $\{q_i + 1\} \subseteq \{l_i\}$. We consider the

normalized difference vector $\mathbf{d}_n^{q_i} = \mathbf{p}^{q_i+1} - \mathbf{p}^{q_i}/\delta^{q_i}$. We have $\mathbf{p}^{q_i+1} = \mathbf{p}^{q_i} + \delta^{q_i}\mathbf{d}_n^{q_i}, \| \mathbf{d}_n^{q_i} \|_2 = 1$ and $\mathbf{d}_n^{q_i}$ differs from zero only along the nth block-component. Here, $\mathbf{d}_n^{q_i}$ belongs to a compact set and has a limit point $\bar{\mathbf{d}}_n$. We assume that $\mathbf{d}_n^{r_i}$ converges to $\bar{d}_n$ by restricting to a further subsequence of $\{r_i\} \subseteq \{q_i\}$.

Then, we consider $\epsilon \in [0, 1]$ and $0 \leq \epsilon \delta_0 \leq \delta^{r_i}$. Thus, $\mathbf{p}^{r_j} + \epsilon \delta_0 \mathbf{d}_n^{r_i}$ lies on the segment joining $\mathbf{p}^{r_i}$ and $\mathbf{p}^{r_i} + \delta_n^{r_i}\mathbf{d}^{r_i}d_n^{r_i} = \mathbf{p}^{r_i+1}$ and it belongs to the compact set $\mathcal{P}$. $\mathbf{p}^{r_i+1}$ maximizes $\mathcal{W}(\cdot)$ over all p which differ from p along the nth block-component. Thus, using the concavity of $\mathcal{W}(\cdot)$, we obtain:

$$\mathcal{W}(\mathbf{p}^{r_i+1}) \geq \mathcal{W}(\mathbf{p}^{r_i+1} + \epsilon \delta_0 \mathbf{d}^{r_i}) \geq \mathcal{W}(\mathbf{p}^{r_i}). \quad (25)$$

Since $\mathcal{W}(\mathbf{p}^{r_i})$ converges to $\mathcal{W}(\mathbf{p}^*)$, $\mathcal{W}(\mathbf{p}^{r_j+1})$ also converges to $\mathcal{W}(\mathbf{p}^*)$. To obtain $\mathcal{W}(\mathbf{p}^*) \geq \mathcal{W}(\mathbf{p}^* + \epsilon \delta_0 \bar{\mathbf{d}}^{r_i}) \geq \mathcal{W}(\mathbf{p}^*)$, we use the limit i tends to infinity. We observe that $\mathcal{W}(\mathbf{p}^*) = \mathcal{W}(\mathbf{p}^{r_i+1} + \epsilon \delta_0 \bar{\mathbf{d}}^{r_i})$ for every $\epsilon \in [0, 1]$. As a function of the nth block component, $\epsilon \delta_0 \bar{\mathbf{d}}^{r_i} \neq 0$ contradicts the strict concavity of $\mathcal{W}(\cdot)$ and it implies that $\mathbf{p}^{r_i} - \mathbf{p}^{r_i}$ converges to zero. In particular, $\mathbf{p}^{r_i+1}$ converges to $\mathbf{p}^*$. Using this approach, for every sequence $\{\mathbf{p}^{q_i}\}$ converging to $\mathbf{p}^*$, the sequence $\{\mathbf{p}^{q_i+K}\}$ also converges to $\mathbf{p}^*$ for all $K \in \mathbb{Z}^+$. We already know that the smart grid predefines the cycle length as N to ensure the convergence of the update process. We consider that $\mathbf{p}^{q_i}$ converges to $\mathbf{p}^*$. Let $\{r_i\}$ be a subsequence of $\{q_i\}$ with $r_{i+1} - r_i > N + K$. If $\mathcal{Z}_{l_i} = \{\mathbf{p}^{q_i}, ..., \mathbf{p}^{q_i+N+K}\}$. As N is the cycle length, the smart grid updates the power amount for each OLEV n such that the amount is updated at least once in $\mathcal{Z}_{l_i}$ times. Let us consider n_i as the OLEV i and its schedule is updated at $\mathcal{Z}_i$ for the first time. Since all the elements in $\mathcal{Z}_i$ converge to $\mathbf{p}^*$, from Equation (21) of the power schedule update process, we have:

$$\mathcal{W}(\mathbf{p}^{q_i+n_i}) \geq \mathcal{W}(\mathbf{p}_n, \mathbf{p}_{-n}^{q_i+n_i-1}), \forall \mathbf{p}_n \in \mathcal{P}_n. \quad (26)$$

Taking the limit as i tends to infinity, we conclude:

$$\mathcal{W}(\mathbf{p}^*) \geq \mathcal{W}(\mathbf{p}_n, \mathbf{p}_{-n}^*), \forall \mathbf{p}_n \in \mathcal{P}_n. \quad (27)$$

Using the first order optimality conditions we obtain:

$$\nabla_n \mathcal{W}(\mathbf{p}^*)(\mathbf{p}_n - \mathbf{p}_n^*) \leq 0, \forall \mathbf{p}_n \in \mathcal{P}_n. \quad (28)$$

where $\nabla_n \mathcal{W} = \frac{\delta \mathcal{W}}{\delta \mathbf{p}_n}$ denotes the partial derivative of $\mathcal{W}(\cdot)$ with $\mathbf{p}_n$ coordinate. From all the inequalities in Equation (28), it concludes that $\nabla \mathcal{W}(\mathbf{p}^*)(\mathbf{p} - \mathbf{p}^*) \leq 0, \forall \mathbf{p} \in \mathcal{P}$ using the Cartesian product structure of the set $\mathcal{D}$. Based on the strictly concavity of $\mathcal{W}(\cdot)$, $\mathbf{p}^*$ maximizes $\mathcal{W}(\cdot)$ over $\mathcal{P}$. $\square$

In next section, we evaluate our propose pricing policy to evaluate its performance.

V. PERFORMANCE EVALUATION

In this section, we evaluated the performance of our proposed game theory-based nonlinear pricing policy in different scenarios and compared with linear pricing policy through simulation study.
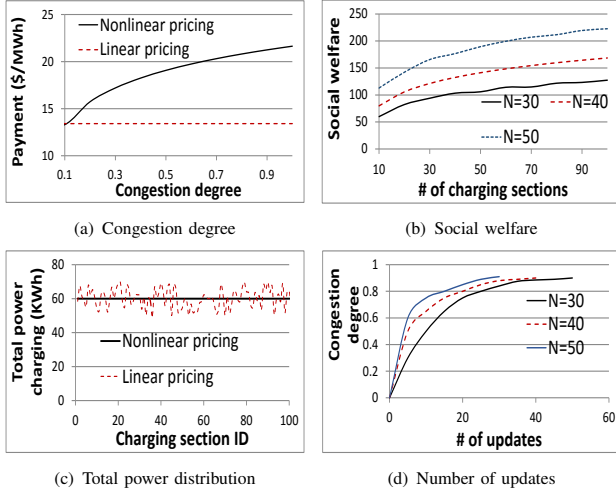
1204

Fig. 5: Results when velocities of OLEVs are 60mph.

(a) Congestion degree (b) Social welfare (c) Total power distribution (d) Number of updates

Fig. 6: Results when velocities of OLEVs are 80mph.

(a) Congestion degree (b) Social welfare (c) Total power distribution (d) Number of updates

A. Experimental Settings

In our simulation, we considered a WPT system where several charging sections share power with the OLEVs using Java programming language. Considering the hourly traffic count of a day of the *NYC* [20], we varied the number of OLEVs from 10 to 50 in each time the smart grid executed the game and we varied the number of chargingsections from 10 to 100. We considered each OLEV has 46.2Ah capacity, 399V regular voltage, 325V cutoff voltage, and 240A current [41]. To ensure the safety and battery life of the OLEVs, SOC of OLEV cannot be lower than SOC_{min} and it cannot be higher than SOC_{max}. According to the average daily driving distance probability distribution obtained from National Household Travel Survey (NHTS), nearly 70% are from 10–30 miles [42]. Thus, we considered OLEVs can receive up to 50% of their SOC from the smart grid based on daily travel distance and SOC requirements. we set SOC_{min} to 0.2 and SOC_{max} to 0.9.

In our game theory-based framework, we assigned the satisfaction function as $\mathcal{U}_n = log(1 + p_n)$ for receiving p_n amount of power for OLEV n. The smart grid sets the power cost for each OLEV to minimize the power charging cost. We considered the nonlinear pricing policy as $\mathcal{V}(p_n) = \beta(\alpha + \frac{p_n}{P^{OLEV}_n})^2$ to determine the power payment function for each OLEV. Also, we considered the linear pricing policy as $\mathcal{V}(p_n) = \beta p_n$ for comparison. We set β equaled to LBMP defined by NYISO [36] and α equaled to 0.875 based on the profit the smart grid wants to make. We assumed that the smart grid determines the power schedules p_n, for on-demand instance OLEVs.

B. Experimental Results

Fig. 5 shows the experiment results when velocities of OLEVs are 60mph and Fig. 6 shows the experiment results when velocities are 80mph. Usually, the speed limit on a freeway is either 80mph in rural areas or 65mph in urban areas. Thus, our considerations of 60mph and 80mph vehicle
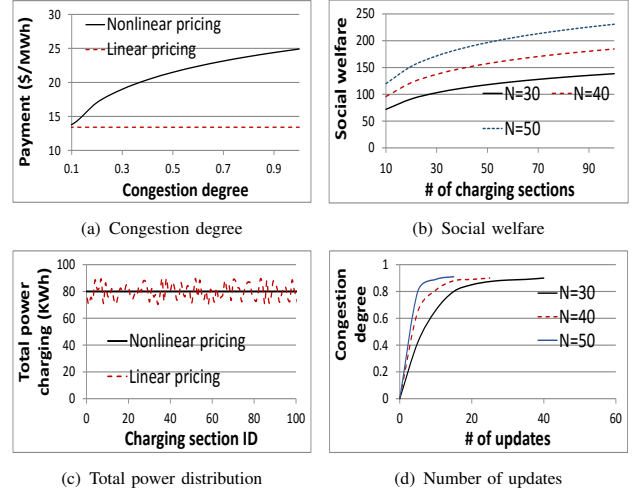
velocities as experimental settings are practical, and these velocities would evaluate the situations when EVs would spend the least possible time on top of charging sections. In the simulation study, at first, we measured the power payment of OLEVs. We varied the desired congestion degree from 0.1 to 1 with step increase of 0.1. The congestion degree represents the percentage of deducted power over the total power capacity on the charging sections. After the optimal power schedule is determined, we calculated the total power payment of OLEVs based on Equation (7). Fig. 5(a) and Fig. 6(a) show the amount of payment with respects to congestion degree when velocities are 60mph and 80mph, respectively. Here, we compared our nonlinear pricing policy with linear pricing policy discussed in Section V-A. As we discussed, using nonlinear pricing policy, the power payment cost increases as the congestion degree increases. Thus, if charging sections are less congested based on their capacity, OLEVs pay less for a specific amount of power. Therefore, the OLEVs request more power when the charging sections are less congested. In contrast, the power payment does not change with the congestion degree when we use linear pricing policy. We also found that higher velocity of OLEVs decreases payment cost as the total amount of power OLEV can receive decreases at the same time. As a result, the congestion degree converges to the desired congestion degree than using the linear pricing policy.

Next, in Fig. 5(b) and Fig. 6(b), we calculated the changes of social welfare when the number of charging sections changes. Here, we changed the number of OLEVs three times (30, 40, and 50) to evaluate the effect of different number of OLEVs on social welfare. We found that the social welfare increases as well as the number of OLEVs increases. It demonstrates that more OLEVs provides better social welfare, i.e., a higher amount of power OLEVs can deduct from charging sections. Through more charging sections, the smart grid is more likely to be more satisfied with the OLEVs. As previous figures, We also noticed the same relationship (more velocity causes more social welfare) between velocity and social welfare.

In Fig. 5(c) and Fig. 6(c), we depicted the total power charging scenarios for nonlinear and linear pricing policies. Here, when OLEV velocity increases, the total power charging from charging sections decreases. The figures show the total charging power from 100 charging sections and when the number of OLEVs was 50 and velocities of OLEVs were approximately equal to 60mph and 80mph, respectively. The simulation resulted from running the best response strategy for 1000 number of updates. Here, the OLEVs compete with each other for available power from charging sections. Using proposed nonlinear pricing policy, at each iteration, the smart grid schedules the power evenly from charging sections and it balances power charging over the charging sections as in Lemma IV.1 to minimize power charging cost for charging sections. This results in the balanced load over charging sections as shown in Fig. 5(c) and Fig. 6(c). Thus, the smart grid balances load over charging sections using nonlinear pricing policy. However, if the smart grid uses linear pricing policy, the smart grid does not distribute power evenly over all charging sections and different charging sections share their power differently with all OLEVs. Thus, load balancing is not maintained strictly if linear pricing policy is applied

Finally, we measured the convergence speed for our nonlinear pricing technique when the desired congestion degree was set to 90%. Here, the convergence speed means how fast the initial power schedule reaches to the optimal power schedule. Figures 5(d) and 6(d) show the congestion degree of OLEVs as the number of updates increases in the simulation. These figures are obtained by taking an average of 50 times of experiment runs. As it is seen, the congestion degree converges faster when the velocity is 60mph, and it needs fewer updates to converge than the case when velocity is 80mph. As we discussed in the previous section, using nonlinear pricing policy, the power payment cost increases as the congestion degree increases. Thus, for the less congested charging sections, OLEVs pay less for a specific amount of power. Therefore, OLEVs request more power when charging sections are less congested. Since the total amount of power provided by OLEVs decreases when velocity increases, the lower velocity of OLEVs causes faster convergence.

VI. Conclusion

We considered a WPT system where charging sections share energy with OLEVs while they are running on the road. We presented a game-theory based pricing framework for opportunistic energy sharing from charging sections to OLEVs such that load balance exists considering energy demand, price, and availability. At first, we evaluated the motivation of this work with a study of opportunistic energy sharing for the WPT systems. We used hourly traffic count of a road section in the *NYC* in *SUMO* to analyze the amount of energy OLEVs can receive at different times of the day. We proposed a distributed power schedule framework to find the optimal schedule between OLEVs and charging sections of the smart grid. The optimal power schedule for OLEVs is selected using a best response-based strategic game. Actually, OLEVs pay

for the power received through charging sections based on the power payment function. We proved that the initial power schedule converges to the optimal power schedule mathematically. As a result, there is load balancing of power sharing procedures among different charging sections. We verified the performance of our proposed pricing policy with respect to the degree of congestion in charging sections, total payment of OLEVs, and the number of update procedures between OLEVs and the smart grid. In future work, we plan to consider optimal deployment of charging sections and communication receivers to benefit both OLEVs and the smart grid. We also plan to consider the effect charging section placement will have on OLEV path planning. Cities may consider dedicating lanes to OLEVs or placing charging sections at traffic lights or stop signals and well-traveled road sections.

VII. Acknowledgements

References

[1] A. EPA, "Inventory of US greenhouse gas emissions and sinks: 1990-2014," EPA 430-R-11-005, Tech. Rep., 2016.

[2] X. Cheng, X. Hu, L. Yang, I. Husain, K. Inoue, P. Krein, R. Lefevre, Y. Li, H. Nishi, J. G. Taiber *et al.*, "Electrified vehicles and the smart grid: The ITS perspective," *IEEE Trans. on ITS*, 2014.

[3] M. Buechel, J. Frtunikj, K. Becker, S. Sommer, C. Buckl, M. Armbruster, A. Marek, A. Zirkler, C. Klein, and A. Knoll, "An automated electric vehicle prototype showing new trends in automotive architectures," in *Proc. of ITSC*, 2015.

[4] M. Honarmand, A. Zakariazadeh, and S. Jadid, "Optimal scheduling of electric vehicles in an intelligent parking lot considering vehicle-to-grid concept and battery condition," *Energy*, 2014.

[5] A. Diaz Alvarez, F. Serradilla Garcia, J. E. Naranjo, J. J. Anaya, and F. Jimenez, "Modeling the driving behavior of electric vehicles using smartphones and neural networks," *IEEE ITS Magazine*, 2014.

[6] "Tesla model 3," https://www.teslamotors.com/model3, [Accessed: December 2016].

[7] A. Sarker, C. Qiu, H. Shen, A. Gil, J. Taiber, M. Chowdhury, J. Martin, M. Devine, and A. Rindos, "An efficient wireless power transfer system to balance the state of charge of electric vehicles," in *Proc. of ICPP*, 2016.

[8] L. Yan, H. Shen, J. Zhao, C. Xu, F. Luo, and C. Qiu, "CatCharger: Deploying wireless charging lanes in a metropolitan road network through categorization and clustering of vehicle traffic," in *Proc. of INFOCOM*, 2017.

[9] E. Romero-Cadaval, F. Barrero-González, E. González-Romera, and M.-I. Milanés-Montero, "Using plug-in electric vehicles to implement ancillary services in smart

distribution grids," in *Plug In Electric Vehicles in Smart Grids*, 2015.

[10] Z. Li, M. Chowdhury, P. Bhavsar, and Y. He, "Optimizing the performance of vehicle-to-grid (V2G) enabled battery electric vehicles through a smart charge scheduling model," *International Journal of Automotive Technology*, 2015.

[11] B. Chen, K. S. Hardy, J. D. Harper, T. P. Bohn, and D. S. Dobrzynski, "Towards standardized vehicle grid integration: Current status, challenges, and next steps," in *Proc. of ITEC*, 2015.

[12] U. K. Madawala and D. J. Thrimawithana, "A bidirectional inductive power interface for electric vehicles in V2G systems," *IEEE Trans. on IE*, 2011.

[13] H. Shen and Z. Li, "New bandwidth sharing and pricing policies to achieve a win-win situation for cloud provider and tenants," *IEEE Trans. on PDS*, 2016.

[14] J. Liu, H. Shen, and L. Chen, "CORP: Cooperative opportunistic resource provisioning for short-lived jobs in cloud systems," in *Proc. of CLUSTER*, 2016.

[15] H. Shen, G. Liu, and H. Wang, "An economical and slo-guaranteed cloud storage service across multiple cloud service providers," *IEEE Trans. on PDS*, 2017.

[16] C. Qiu, H. Shen, and L. Chen, "Towards green cloud computing: Demand allocation and pricing policies for cloud service brokerage," in *Proc. of Big Data*, 2015.

[17] W. Tushar, W. Saad, H. V. Poor, and D. B. Smith, "Economics of electric vehicle charging: A game theoretic approach," *IEEE Trans. on SC*, 2012.

[18] Z. Fan, "A distributed demand response algorithm and its application to phev charging in smart grids," *IEEE Trans. on SC*, 2012.

[19] T. Cui, Y. Wang, S. Chen, Q. Zhu, S. Nazarian, and M. Pedram, "Optimal control of PEVs for energy cost minimization and frequency regulation in the smart grid accounting for battery state-of-health degradation," in *Proc. of ADAC*, 2015.

[20] "New York City Department of Transportation," http://www.nyc.gov/html/dot/html/about/datafeeds.shtml, [Accessed: December 2016].

[21] L. Kang, H. Shen, and A. Sarker, "Velocity optimization of pure electric vehicles with traffic dynamics consideration," in *Proc. of ICDCS*, 2017.

[22] A. Sarker, C. Qiu, and H. Shen, "A decentralized network with fast and lightweight autonomous channel selection in vehicle platoons for collision avoidance," in *Proc. of MASS*, 2016.

[23] ——, "Quick and autonomous platoon maintenance in vehicle dynamics for distributed vehicle platoons," in *Proc. of IoTDI*, 2017.

[24] C. Qiu, H. Shen, A. Sarker, V. Soundararaj, M. Devine, and E. Ford, "Towards green transportation: Fast vehicle velocity optimization for fuel efficiency," in *Proc. of IEEE CloudCom*, 2016.

[25] L. Yan and H. Shen, "TOP: vehicle trajectory based driving speed optimization strategy for travel time minimization and road congestion avoidance," in *Proc. of MASS*, 2016.

[26] L. Yan, H. Shen, and K. Chen, "MobiT: A distributed and congestion-resilient trajectory based routing algorithm for vehicular delay tolerant networks," in *Proc. of IoTDI*, 2017.

[27] Y. Hori, "Future vehicle society based on electric motor, capacitor and wireless power supply," in *Proc. of IPEC*, 2010.

[28] O. C. Onar, J. M. Miller, S. L. Campbell, C. Coomer, C. White, L. E. Seiber *et al.*, "A novel wireless power transfer for in-motion EV/PHEV charging," in *Proc. of APEC*, 2013.

[29] S. Lukic and Z. Pantic, "Cutting the cord: Static and dynamic inductive wireless charging of electric vehicles," *IEEE Electrification Magazine*, 2013.

[30] S. Li and C. C. Mi, "Wireless power transfer for electric vehicle applications," *IEEE Jorunal of Emerging and Selected Topics in Power Electronics*, 2015.

[31] J. Huh, S. W. Lee, W. Y. Lee, G. H. Cho, and C. T. Rim, "Narrow-width inductive power transfer system for online electrical vehicles," *IEEE Trans. on PE*, 2011.

[32] J. Shin, S. Shin, Y. Kim, S. Ahn, S. Lee, G. Jung, S.-J. Jeon, and D.-H. Cho, "Design and implementation of shaped magnetic-resonance-based wireless power transfer system for roadway-powered moving electric vehicles," *IEEE Trans. on IE*, 2014.

[33] Y. D. Ko and Y. J. Jang, "The optimal system design of the online electric vehicle utilizing wireless power transmission technology," *IEEE Trans. on ITS*, 2013.

[34] S. He, Z. Lu, X. Wen, Z. Zhang, J. Zhao, and W. Jing, "A pricing power control scheme with statistical delay QoS provisioning in uplink of two-tier ofdma femtocell networks," *Mobile Networks and Applications*, 2015.

[35] C. D. White and K. M. Zhang, "Using vehicle-to-grid technology for frequency regulation and peak-load reduction," *Journal of Power Sources*, 2011.

[36] "New york independent system operator," http://www.nyiso.com/public/index.jsp, [Accessed: December 2016].

[37] D. Krajzewicz, J. Erdmann, M. Behrisch, and L. Bieker, "Recent development and applications of SUMO - Simulation of Urban MObility," *International Journal On ASM*, 2012.

[38] W. Kempton and J. Tomić, "Vehicle-to-grid power fundamentals: Calculating capacity and net revenue," *Journal of power sources*, 2005.

[39] D. P. Bertsekas, "Nonlinear programming," 1999.

[40] M. J. Osborne and A. Rubinstein, *A course in game theory*. MIT press, 1994.

[41] "Chevrolet-Spark," www.chevrolet.com/Spark, [Accessed: December 2016].

[42] "Summary of travel trends, NHTS," http://nhts.ornl.gov/2009/pub/stt.pdf, [Accessed: December 2016].

1207